Open Access Journal
International Journal of Medical Research and Pharmaceutical Sciences
Volume 3 (Issue 6) : June 2016 ISSN: 2394-9414
DOI: 10.5281/zenodo.55493 Impact Factor- 3.109

CHEMOSENSITATION OF URSOLIC ACID LOADED POLY (LACTIC-CO-GLYCOILC ACID) NANOPARTICLES AND CAFFIENE LOADED POLY (LACTIC-CO-GLYCOILC ACID) NANOPARTICLES IN HT29 CELL LINES

Jose Merlin J.P[*1], Venkadesh B[2], Sheeja S Rajan[3] and Sumesh S[4]

[*1,2]PG & Research Department of Zoology, Muslim arts college, Thiruvithancode, Tamilnadu, India.
[3]Department of Biochemistry, Theivanai Ammal College for Women Villupuram, Tamilnadu, India.
[4]BIOGENIX Research Centre Poojapura, Trivandrum, Kerala, India.

Corresponding author: Mr. J.P Jose Merlin, PG & Research Department of Zoology, Muslim arts college, Thiruvithancode-629 174. Tamilnadu, INDIA.Mobile No. : +91 9442094520

Keywords:
Nanoparticles, Anticancer, Ursolic acid (UA), Caffeine (Caf), Poly lactic-co-glycolic acid (PLGA).

Abstract

The aim of the present study was to develop UA-PLGA NPs and Caf-PLGA NPs to study its anticancer efficacy in HT29 cells in vitro. The method used for the study was to synthesis the nanoparticles, Particle size, size distribution and zeta potential, Drug encapsulation efficiency and in vitro drug release. Then the nanoparticles were subjected in cancer cell lines and the parameters used were Drug treatment and dose fixation study, Apoptotic morphological changes. The results indicate that the chemosensitation of drug loaded nanoparticles demonstrated increased anticancer property in cancer cells than UA-PLGA NPs and Caf-PLGA NPs treatment alone.

INTRODUCTION

Colorectal cancer is the fourth most frequently diagnosed cancer and the second leading cause of cancer death. About 96,830 new cases of colon cancer and approximately 40,000 cases of rectal cancer will occur and 50,310 people will die of colon and rectal cancer combined [1]. The long term survival rate of colon cancer patients treated by conventional modalities such as surgery, radiation, and chemotherapy remains far from satisfactory [2]. Colon cancer cells are only the modestly responsive or even nonresponsive to the cytotoxic effects of chemotherapeutic agents [3].

The term “chemosensitization” was originally introduced as a strategy to counter the development of resistance in tumor cells to anticancer chemotherapeutic agents. Simply put, chemosensitization in cancer therapy involves use of a chemical that renders can- cer cells more sensitive to a chemotherapeutic agent. Development of resistance in cancer cells to anticancer drugs involvedmutations in target genes, up-regulation or over-expression of genes control- ling efflux pumps, production of enzymes that “detoxified” the drugs, and DNA repair [4].

Ursolic acid, a pentacyclic triterpenoid carboxylic acid found in plants, has various biological properties, including anti-inflammatory, anticancer, anti-angiogenic, and antioxidative activities [5, 6]. Numerous reports of UA’s in vitro activities against tumor cell lines have appeared in the literature [7] and the possible mechanisms of action have been reviewed recently [8].

Volume 3 (Issue 6) : June 2016 ISSN: 2394-9414
DOI: 10.5281/zenodo.55493 Impact Factor- 3.109

Caffeine (1, 3, 7-trimethylxanthine) is found in both coffee and tea, so a great number of people are exposed to various doses of caffeine. It acts as a stimulant for the central nervous, respiratory and cardiac system. Caffeine significantly reduces cancer risk caused by environmental and dietary carcinogens [9] and the protective action of caffeine against a variety of chemical carcinogens was established by several studies, carried out by Abraham [10]. Because of purine nature it has a mutagenic potential. The mutagenic effect of caffeine was detected by Fries and Kihlman [11].

Nanotechnology has led to the development of drug delivery systems to achieve the targeted transport of anticancer drugs [12]. Incorporation of anticancer drugs into the nanoparticles, reduces the adverse reactions and increases the therapeutic efficacy due to changes in the pharmacokinetics or tissue distribution [13]. Nanoparticles may be delivered to specific sites by size dependant passive targeting or by active targeting [14, 15]. The passive enhanced permeability and retention (EPR) effect is thought to occur in solid tumors. Vascular endothelial growth factor (VEGF) stimulates vascular endothelial cell growth, increases the permeability of tumor-associated neo vasculature, and causes leakage of circulating macromolecules and small particles into the tumor [16]. Since tumors lack an effective lymphatic drainage system to clear these extravagated substances macromolecules and nanoparticles that enter the tumor has been accumulated [17-19].

PLGA poly (lactic-co-glycolic acid) is one of the most successfully used biodegradable nanosystem for the development of nanomedicines because it undergoes hydrolysis in the body to produce the biodegradable metabolite monomers, lactic acid and glycolic acid [20]. PLGA have potential because of their size, hydrophobic core with hydrophilic periphery, and biocompatibility [21]. In order to minimize systemic toxicity and to improve therapeutic efficacy, in this study we encapsulated UA-PLGA NPs and Caf-PLGA NPs and tested its anticancer potential in colon cancer cells *in vitro*.

MATERIALS AND METHODS

2.1. Chemicals

Poly lactic-co-glycolic acid (PLGA) 65:35 (MW 40,000-75,000), poly vinyl alcohol (PVA) (MW 25,000), Ursolic acid (UA), Caffeine (Caf), thiobarbituric acid (TBA), phenazine methosulphate (PMS), nitroblue tetrazolium (NBT), 5, 5-dithiobis 2-nitrobenzoic acid (DTNB), 3-(4,5-dimethylthiazol-2-yl)-2,5-diphenyl tetrazolium bromide (MTT), ethidium bromide (EtBr), acridine orange (AO), fetal calf serum (FCS), DMEM medium, glutamine-penicillin-streptomycin solution, ficoll-histopaque 1077, trypsin-EDTA were purchased from Sigma Chemicals Co., St. Louis, USA.

2.2. Preparation and characterization nanoparticles

2.2.1. Preparation of drug loaded nanoparticles

UA-PLGA NPs and Caf-PLGA NPs were prepared by nanoprecitation method as previously described by Peltonen, 2003 [2]. 0.1% of PVA was prepared by dissolving 100 mg of PVA in 100 ml distilled water in magnetic stirrer at 60 ºC. Organic solution of PLGA (100 mg) and UA/Caf (10 mg) in acetone (10 ml) was added to PVA solution (10 ml). The sample was sonicated at 25 watts for 2 min (Sonics VC-130, Sonics and Materials Inc. CT, USA) and kept the sample under magnetic stirrer at room temperature for 6 h. To remove the non-incorporated drug, the obtained nanosuspension was centrifuged and washed with distilled water twice at 14,000 rpm for 30 min. The supernatant containing the free drug was discarded and the pellet was freeze dried at
-50 ºC.

2.2.2. Particle size, size distribution and zeta potential

DLS (Zetasizer Nano, Malvern Instruments Ltd. United Kingdom) was used to measure the average size and size distribution of the prepared nanoparticles. Three different batches were analyzed to give an average value and standard deviation for the particle diameter and zeta potential.

Open Access Journal
International Journal of Medical Research and Pharmaceutical Sciences
Volume 3 (Issue 6) : June 2016 ISSN: 2394-9414
DOI: 10.5281/zenodo.55493 Impact Factor- 3.109

2.2.3. Scanning electron microscopy (SEM)

The morphological features of RSV-GNPs were examined by scanning electron microscopy (Quanta 200F, FEI, Hillsboro, OR, USA). The samples were sprinkled onto a double-sided tape and sputter-coated with a 5 nm thick gold layer. The inner-structure of nanoparticles was observed after fracturing by a razor blade.

2.2.4. Differential scanning calorimetry (DSC)

Thermal properties of polymers and particles were measured by DSC. Nitrogen was used as the purge gas. Top pierced aluminum pans were used throughout the study with sample weights varied between 5 and 10 mg. The DSC system was controlled by DSC-Q-200-TA instruments USA, Built 79 software (version 23.10). Samples were characterized by DSC in the range of 25–360˚ C at a heating rate of 10˚C per minute.

2.2.5. Drug encapsulation efficiency

Drug encapsulation efficiency was described by the method of Mathew, 2010 [23]. UA-PLGA NPs and Caf-PLGA NPs were centrifuged at 14,000 rpm for 30 min. The supernatant containing unencapsulated drug was removed. The samples were washed with deionised water and the pellets obtained were re-suspended in deionised water and freeze dried for 48 h to get powdered sample. Three mililitre of the supernatant obtained after centrifugation was taken in a cuvette and the absorbance value was recorded at 266 nm using a UV spectrophotometer.

Encapsulation efficiency (%) = [Drug] tot − [Drug] free / [Drug] tot × 100

2.2.6. In vitro drug release

Drug release profiles of nanoparticles were investigated in PBS and 10 % FBS medium at pH 7.4 accordingly by the method of Dong, 2004 [24]. Five microgram of lyophilized UA-PLGA NPs and Caf-PLGA NPs were dispersed in 30 ml of 10% FBS/PBS and placed in water bath shaker set at 37 ºC with a shaking speed of 120 rpm. At 1h time intervals 3 ml of supernatant from the sample was taken for analysis and the same amount of fresh 10% FBS/PBS was replaced to the sample. Each time absorbance value at 266 nm was recorded using UV spectrophotometer.

$$\text{Drug release (\%)} = \frac{[\text{UA/Caf}]_{rel}}{[\text{UA/Caf}]_{tot}} \times 100$$

2.2.7. Analysis of drug loaded nanoparticles uptake by fluorescence microscopy

The cellular uptake of UA-PLGA NPs and Caf-PLGA NPs in HT29 cells was analyze by the fluorescence microscopy [25]. In brief, cells were incubated with Hoechst 33258 dye (50 mg/mL; blue fluorescence) for 30 min, and then washed two times with PBS. The washed cells were resuspended in media and then incubated with RSV for 3 h. Cells were then examined under a fluorescence microscope (BX51; Olympus, Tokyo, Japan) and images were captured using a Photometrics Cool- snap SHC-745 color camera (Samsung, Korea).

2.3. Anticancer efficacy of drug loaded nanoparticles

Volume 3 (Issue 6) : June 2016 ISSN: 2394-9414
DOI: 10.5281/zenodo.55493 Impact Factor- 3.109

2.3.1 Cell lines and culture conditions

The present work was carried out in colon cancer cell lines (HT29). HT29 cells were obtained from National Centre for Cell Science (NCCS), Pune, India. The present work has been approved by Institutional Ethical Committee(IEC), BIOGENIX Research Centre, Trivandrum. The cells were grown as monolayer in DMEM medium supplemented with 10% FCS, 1mM sodium pyruvate, 10 mM HEPES, 1.5 g/L sodium bicarbonate, 2mM L-glutamine, and 100 U/ml penicillin-streptomycin at 37 C in 5% CO_2 incubator.

2.3.2. Drug treatment and dose fixation study

Cells were treated with different concentration of UA-PLGA NPs and Caf-PLGA NPs (6.25, 12.5, 25, 50 and 100 µg) and incubated for 24 h at 5 % CO_2 incubator. Cytotoxicity was observed by MTT assay by the method of Mosmann, 1983 [26].IC_{50} was calculated by (ED50plus software V 1.0). IC_{50} values were calculated and the optimum dose was used for further study.

2.3.3. Experimental groups

The HT29 cells were divided into 4 experimental groups. Group 1: Untreated control cells, Group 2: UA-PLGA NPs treatment alone (88.10 µg), Group 3: Caf-PLGA NPs treatment alone (49.63 µg) and Group 4: UA-PLGA NPs (88.10 µg) + (after one hour) Caf-PLGA NPs (49.63 µg) treatment.

2.3.4. Apoptotic morphological changes

Apoptotic morphological changes during UA-PLGA NPs and Caf-PLGA NPs treatment were analyzed by AO/EtBr staining. This dual staining method differentiate condensed chromatin of dead apoptotic cells from the intact normal cell nuclei (Lakshmi, 2008) [27].

2.3.5. Erythrocyte aggregation assay

Fresh blood was isolated and added to an equal volume of buffer containing PBS and 10 mM EDTA. Erythrocytes were pelleted by centrifugation, washed multiple times with PBS. To one volume of fresh erythrocytes one volume of UA-PLGA NPs or Caf-PLGA NPs were added. Solutions were incubated for 1 h at 37 ◦C and placed into a 96 well plate for phase contrast imaging [25].

2.6. Statistical analysis

Statistical analysis was performed by one-way ANOVA followed by DMRT taking $p<0.05$ to test the significant difference between groups.

RESULTS

3.1. Physicochemical characterization of drug loaded nanoparticles

It has been noticed that the prepared UA-PLGA NPs and Caf-PLGA NPs possess average size of 120 nm and 100 nm and polydispersity index (PI) of 0.060 and 0.054 (Fig. 1a and b). Further, the prepared UA-PLGA NPs and Caf-PLGA NPs had zeta potential of −24.8 mV and −14.3 mV. It has been found that 69 % of UA and 78 % of Caf were encapsulated in PLGA NPs (Table 1). SEM images of the UA-PLGA NPs and Caf-PLGA NPs are shown in Fig. 2. The prepared UA-PLGA NPs and Caf-PLGA NPs had smooth surface but with some irregular small particles. Further, there was no drug melting peak observed in the DSC curve for UA-PLGA NPs and Caf-PLGA NPs are shown in Fig. 3 a and b.

Open Access Journal
International Journal of Medical Research and Pharmaceutical Sciences
Volume 3 (Issue 6) : June 2016 ISSN: 2394-9414
DOI: 10.5281/zenodo.55493 Impact Factor- 3.109

3.2. Drug encapsulation efficiency and in vitro drug release

Table 1 shows the amount of drug encapsulated in PLGA nanosystem. The encapsulation efficiencies of UA-PLGA NPs and Caf-PLGA NPs are in the range of 69 % and 78 %. Figure 4 shows the % drug release in PBS during different time interval. After 3 h incubation, 7 % of UA and 9 % of Caf was released in the PBS and the maximum of 69 % of UA and 82 % of Caf release were observed upon 30 h incubation. Upon incubation with 10% FBS, 7% and 69% UA was released in 3h and 30 h and 9 % and 82% Caf was released in 3 h and 30 h respectively.

3.3. Uptake of drug loaded nanoparticles by HT29 cells

Visual evidence of UA-PLGA NPs and Caf-PLGA NPs uptake by the HT29 cells during 30 min incubation time was analyzed by fluorescence microscopy using Hoechst 33258 dye. UA-PLGA NPs and Caf-PLGA NPs treated cells show brighter fluorescence due to enhanced intracellular uptake (Fig. 5).

3.4. Drug treatment and dose fixation study

Figure 6 shows the % cytotoxicity of UA-PLGA NPs and Caf-PLGA NPs (6.25, 12.5, 25, 50 and 100 µg) in HT29 cells. Inhibitory concentration 50 (IC_{50}) value for UA-PLGA NPs and Caf-PLGA NPs was found to be 88.10 µg and 49.63 µg respectively, and it was used for further experiments.

3.5. Effect of drug loaded nanoparticles on apoptotic morphology

Figure 7a shows the photomicrographs of apoptotic morphological changes in UA-PLGA NPs, Caf-PLGA NPs and UA-PLGA NPs + Caf-PLGA NPs treated cells. The % apoptotic cell death was increased during UA-PLGA NPs, Caf-PLGA NPs and UA-PLGA NPs + Caf-PLGA NPs treatment. It was found that treated cells showed 64%, 87 % and 93% of apoptotic cells, respectively (Figure 7b).

3.6. Erythrocyte aggregation assay

The control caused no effect in aggregation of erythrocytes upon 1 h incubation at room temperature, like that UA-PLGA NPs and Caf-PLGA NPs have not showed any effect with the erythrocytes was shown in figure 8.

DISCUSSION

Ursolic acid has various biological properties, including anti-inflammatory, anticancer, anti-angiogenic, and antioxidative activities [5, 6]. Caffeine is found in both coffee and tea, so a great number of people are exposed to various doses of caffeine. Caffeine significantly reduces cancer risk caused by environmental and dietary carcinogens [9]. Increase in the specific surface area caused by the formation of smaller nanodroplets during the emulsification stage of the process, may facilitate the diffusion of the drug to the external phase along with the solvent, leading to incorporation efficiencies [28, 29].

The physicochemical characteristics of colloidal systems, namely size and surface morphology, are recognized to affect their physical stability and to significantly influence their interaction with the release rate of an incorporated drug and their interaction with cells [30, 31]. The method used in this work allowed the instantaneous and reproducible formation of UA-PLGA NPs exhibiting diameters below 120 nm and low polydispersity indexes, indicating an homogeneous size distribution. The mean zeta potential of UA-PLGA NPs exhibited a negative value of -24.8±0.4 mV and Caf-PLGA NPs exhibiting diameters below 100 nm and low polydispersity indexes, indicating an homogeneous size distribution. The mean zeta potential of Caf-PLGA NPs exhibited a negative value of -14.3±0.5 mV. The melting endothermic peak of pure UA appeared at 278.8˚C and the peak of Caf appeared at 257.4˚C. However no melting was detected for both nanoparticle formulations. Thus, it can be concluded that UA in

Volume 3 (Issue 6) : June 2016 ISSN: 2394-9414
DOI: 10.5281/zenodo.55493 Impact Factor- 3.109

the nanoparticle and Caf in the nanoparticle were in an amorphous or disordered crystalline or in the solid solution state.

Further, we noticed that the PLGA degraded gradually and released the drug in a sustained manner. 7 % UA was released in 3h and 69 % UA was released in 30 h incubation in the PBS and 9 % Caf was released in 3h and 82 % Caf was released in 30 h incubation in the PBS. This result indicates that the prepared nanoparticles are useful for controlled delivery system for cancer treatment [32]. UA-PLGA NPs and Caf-PLGA NPs/Hoechst 33258 entered the cells during the incubation period and the fluorescence was found inside the nuclei, which indicate that UA-PLGA NPs and Caf-PLGA NPs might prove to be useful in site specific delivery of drugs whose site of pharmacological activity might be the cell nucleus, which has been evidenced by diminished fluorescence observed in Fig. 5.

Furthermore, we evaluated the anticancer activity of UA-PLGA NPs and Caf-PLGA NPs in HT29 cell line. It was found that UA-PLGA NPs and Caf-PLGA NPs could greatly inhibit the HT29 cell growth. The reason for increased cytotoxicity observed in the UA-PLGA NPs and Caf-PLGA NPs group might be due to increased cellular uptake and sustained drug delivery. Enhanced cytotoxicity during UA-PLGA NPs and Caf-PLGA NPs treatment indicates that PLGA has the potency to transport more UA and Caf into the cells, thus achieving greater cytotoxicity. IC_{50} values for UA-PLGA NPs and Caf-PLGA NPs in our study were 88.10 µg and 49.63 µg. Previously 88.69 µM value reported before for PTX [33].

It has been previously demonstrated that RSV induced apoptosis in EC-9706 cells with typical apoptotic characteristics includes chromatin condensation, nucleus fragmentation and apoptotic body formation [34]. The increased apoptotic incidence during UA-PLGA NPs and Caf-PLGA NPs treatments clearly indicates the enhanced anticancer potential of UA-PLGA NPs and Caf-PLGA NPs combination (Fig. 8). Similar to these findings a 10-times reduction in hemolysis of erythrocytes during GNP-amphotericin-B treatment when compared with plain amphotericin-B [35].

We have observed UA-PLGA NPs + Caf-PLGA NPs pretreatment significantly increased apoptotic morphological changes in HT29 cells than UA-PLGA NPs and Caf-PLGA NPs treatment alone. Apoptosis has been shown to be a significant mode of cell death after cytotoxic drug treatment [36]. Further studies warrants to explore the merits of UA-PLGA NPs + Caf-PLGA NPs for cancer chemotherapy.

DISCLOUSURE OF INTEREST

The authors declare that they have no conflicts of interest concerning this article.

REFERNECES

[1] *Siegel R, Ma J, Zou Z, Jemal A. Cancer statistics. CA Cancer J Clin, 2014, 64, 9-29.*
[2] Tseng C.L, Su W.Y, Yen K.C, Yang K.C, Lin F.H, The use of biotinylated-EGF- modified gelatin nanoparticle carrier to enhance cisplatin accumulation in cancerous lungs via inhalation, Biomaterials, 2009, 30, 3476–3485.
[3] D'Angelillo R.M, Trodella L, Ciresa M, Cellini F, Fiore M, Greco C. Multimodality treatment of stage III non-small cell lung cancer: analysis of a phase II trial using preoperative cisplatin and gemcitabine with concurrent radiotherapy. J Thorac Oncol, 2009, 4, 1517-23.
[4] Shabbits J.A, HuY and Mayer L. D. Tumor chemosensitization strategies based on apoptosis manipulations. Mol.CancerTher, 2003, 2, 805–813.
[5] Zheng Q.Y, Jin F.S, Yao C, Zhang T, Zhang G.H, Ai X. Ursolic acid-induced AMP activated protein kinase (AMPK) activation contributes to growth inhibition and apoptosis in human bladder cancer T24 cells. Biochem Biophys Res Commun 2012, 419, 741-7.

Volume 3 (Issue 6) : June 2016 ISSN: 2394-9414
DOI: 10.5281/zenodo.55493 Impact Factor- 3.109

[6] Limami Y, Pinon A, Leger DY, Mousseau Y, Cook-Moreau J, Beneytout JL et al. HT- 29 colorectal cancer cells undergoing apoptosis overexpress COX-2 to delay ursolic acid-induced cell death. Biochimie 2011, 93, 749-57.

[7] Novotny L, Vachalkova A, Biggs D. Ursolic acid: an anti-tumorigenic and chemopreventive activity minireview. Neoplasma, 2001, 48, 241–246.

[8] Neto C.C. Cranberry and its phytochemicals: a review of in vitro anticancer studies. J Nutr, 2007, 137, 186–193.

[9] Kesavan P.C. Oxygen effect in radiation biology: Caffeien and serendipity. Current Science, 2005, 89(2), 318-328.

[10] Abraham S.K. Inhibitory effects of coffee on the genotoxicity of carcinogens in mice. Mutation Research, 1991, 262, 109-114.

[11] Fries N, Kihlman B. Fungal mutations obtained with methyl xanthines. Nature, 1948, 162, 573.

[12] Caddeo C, Teska K, Sinico C, Kristl J. Effect of resveratrol incorporated in liposomes on proliferation and UV-B protection of cells International Journal of Pharmcology, 2008, 363, 183–191.

[13] Leroux J.C, Doelker E, Gurny R. The use o obtained f drug-loaded nanoparticles in cancer chemotherapy. In: Benita S, editor. Microencapsulation. New York: Marcel Dekker, 1996, 535-75.

[14] Matsumura Y, Maeda H. A new concept for macromolecular therapeutics in cancer chemotherapy: mechanism of tumoritropic accumulation of proteins and the antitumor agent smancs. Cancer Res, 1986, 46, 6387–92.

[15] Hashida M, Akamatsu K, Nishikawa M, Yamashita F, Takakura Y. Design of polymeric prodrugs of prostaglandin E1 having galactose residue for hepatocyte targeting. J Control Release, 1999, 62, 253–62.

[16] Nori, A, Kopecek, J. 2005. Intracellular targeting of polymer-bound drugs for cancer chemotherapy. Adv. Drug Deliv. Rev, 57, 609–636.

[17] Peterson, C.M., Shiah, J.G., Sun, Y., Kopeckova, P., Minko, T., Straight, R.C., Kopecek, J.,2003. HPMA copolymer delivery of chemotherapy and photodynamic therapy in ovarian cancer. Adv. Exp. Med. Biol, 519, 101–123.

[18] Torchilin, V.P., Lukyanov, A.N., 2003. Peptide and protein drug delivery to and into tumors: challenges and solutions. Drug Discov. Today, 8, 259–266.

[19] Gao, X., Cui, Y., Levenson, R.M., Chung, L.W., Nie, S., 2004. In vivo cancer targeting and imaging with semiconductor quantum dots. Nat. Biotechnol, 22, 969–976.

[20] Cho K, Wang X, Nie S, Chen ZG, Shin DM. Therapeutic nanoparticles for drug delivery in cancer. Clinical Cancer Research, 2008, 14, 1310–6.

[21] Gomez-Gaete C. Encapsulation of dexamethasone into biodegradable polymeric nanoparticles. International Journal of Pharmacology, 2007, 331, 153–159.

[22] Peltonen L, Koistinen P, Hirvonen J. Preparation of nanoparticles by the nanoprecipitation of low molecular weight poly(l)lactide. STP Pharma Sci. 2003, 13, 299-304.

[23] Mathew M.E, Mohan J.C, Manzoor K, Nair S.V, Tamura H, Jayakumar R, Folate conjugated carboxymethyl chitosan-manganese doped zinc sulphide Nanoparticles for targeted drug delivery and imaging of cancer cells, Carbohydrate polymers 80, (2010), 443-449.

[24] Dong Y, Feng SS. Methoxy poly(ethylene glycol)-poly(lactide) (MPEG-PLA) nanoparticles for controlled delivery of anticancer drugs. Biomaterials, 2004, 2843-9.

[25] Karthikeyan S, Prasad N.R, Gnanamani, Balamurugan E. Anticancer activity of resveratrol-loaded gelatin nanoparticles on NCI-H460 non-small cell lung cancer cells. Biomedicine and preventive nutrition, 2013, 3(1), 64-73.

[26] Mosmann T, Rapid calorimetric assay for cellular growth and survival: application of proliferation and cytotoxicity assay, J Immol. Methods, 65 (1-2), (1983), 55-63.

[27] Lakshmi S, Dhanaya G.S, Joy B, Padmaja G, Remani P. Inhibitory effect of an extract of Curcuma Zedoariae on human cervical carcinoma cells. Med Chem Res, 2008, 17, 335-44.

[28] Bodmeier R, Maincent P, Polymeric dispersions as drug carriers, in: H.A. Lieberman, M.M. Rieger, G.S. Banker (Eds.), Pharmaceutical Dosage Forms: Disperse Systems, Marcel Dekker, New York, 1998, 3, 87–127.

[29] Govender T, Stolnik S, Garnett M.C, Illum L, Davis S.S. PLGA nanoparticles prepared by nanoprecipitation: drug loading and release studies of a water soluble drug, J. Control. Release, 1999, 57 (2), 171–185.

Volume 3 (Issue 6) : June 2016 ISSN: 2394-9414
DOI: 10.5281/zenodo.55493 Impact Factor- 3.109

[30] Pauillard V, Nicolaou A, Double J.A, Philips R.M. Methionine dependence of tumours : a biochemical strategy for optimizing paclitaxel chemosensitivity in vitro. Biochem Pharmacol, 2006, 71, 772-8.
[31] Halliwell B, Gutteridge J.M.C. Free radicals in biology and medicine. Oxford: Clarendon Press, 1989.
[32] Hildeman D.A, Mitchell T, Teague T.K, Henson P, Day B.J, Kappler J, and Marrack P.C. Reactive oxygen species regulate activation-induced T cell apoptosis. Immunity, 1999, 10, 735-744.
[33] Zhang M, Boyer M, Rivory L, Hong A, Clarke S, Stevens G, Fife K. Radiosensitization of vinorelbine and gemcitabine in NCI-H460 non–small-cell lung cancer cells. Int J Radiat Oncol Biol Phys, 2004, 58(2), 353–360.
[34] Zhou H.B, Yan Y, Sun Y.N, Zhu J.R. Resveratrol induces apoptosis in human esophageal carcinoma cells. World J Gastroenterol 2003, 9, 408–11.
[35] Manoj N, Dinesh M, Dubey V, Jain N.K. Development, characterization, and toxicity evaluation of amphotericin B – loaded gelatin nanoparticles. Nanomedicine 2008, 4, 252–61.
[36] Mcmillan T.J, Steel G.G. DNA damage and cell killing. In: Steel GG (eds) Basic Clin Radiol London, 1997, 58-69.

LIST OF LEGENDS

Table 1: Shows the drug encapsulation efficiency, polydispersity index, size and surface charge of the UA-PLGA NPs and Caf-PLGA NPs.

Figure 1 a: Shows the size distribution of UA-PLGA NPs by DLS.

Figure 1 b: Shows the size distribution of Caf-PLGA NPs by DLS.

Figure 2: Shows the morphology of UA-PLGA NPs and Caf-PLGA NPs by SEM.

Figure 3 a: Show the thermal gravitometric curve of UA-PLGA NPs

Figure 3 b: Show the thermal gravitometric curve of Caf-PLGA NPs

Figure 4: Shows the percentage of UA and Caf released from PLGA nanoparticles during different time intervals in 10% FBS/PBS. Values are given as mean ± S.D. of six experiments in each group.

Figure 5: Cellular uptake of UA-PLGA NPs and Caf-PLGA NPs by HT29 cells. Microscopic images (Hoechst staining) of HT29 cells incubated with UA-PLGA NPs and Caf-PLGA NPs: Enhanced staining indicates improved cellular uptake of UA-PLGA NPs and Caf-PLGA NPs.

Figure 6: Optimum dose fixation study by MTT assay. (IC_{50}) value for UA-PLGA NPs and Caf-PLGA NPs was found to be 88.10 µg and 69.63 µg, respectively. Values are given as mean ± S.D. of six experiments in each group.

. Figure 7 a: Orange-red color indicates the occurrence of apoptosis, while green color indicates the absence of apoptosis in HT29 cells.

Figure 7 b: Percentage apoptotic cell death was increased in UA-PLGA NPs and Caf-PLGA NPs treated cells. Values are given as mean ± S.D. of six experiments in each group.

Figure 8: Shows the bright field micrograph of RBC aggregation of control, UA-PLGA NPs and Caf-PLGA NPs.

Open Access Journal
International Journal of Medical Research and Pharmaceutical Sciences
Volume 3 (Issue 6) : June 2016 ISSN: 2394-9414
DOI: 10.5281/zenodo.55493 Impact Factor- 3.109

Table 1

Fabrications variables		Encapsulation Efficiency (%)	Mean Diameter (nm)	Polydispersity index	Size (nm)	Zeta potential (mV)
Polymer	Drug					
PLGA	UA	69 ± 0.21	145.2 ± 80.3	0.060 ± 0.11	120 ± 4.8	-24.8 ± 0.4
PLGA	Caf	78 ± 4.36	133.6 ± 39.5	0.054 ± 0.09	100 ± 4.3	-14.3 ± 0.5

Fig 1 a

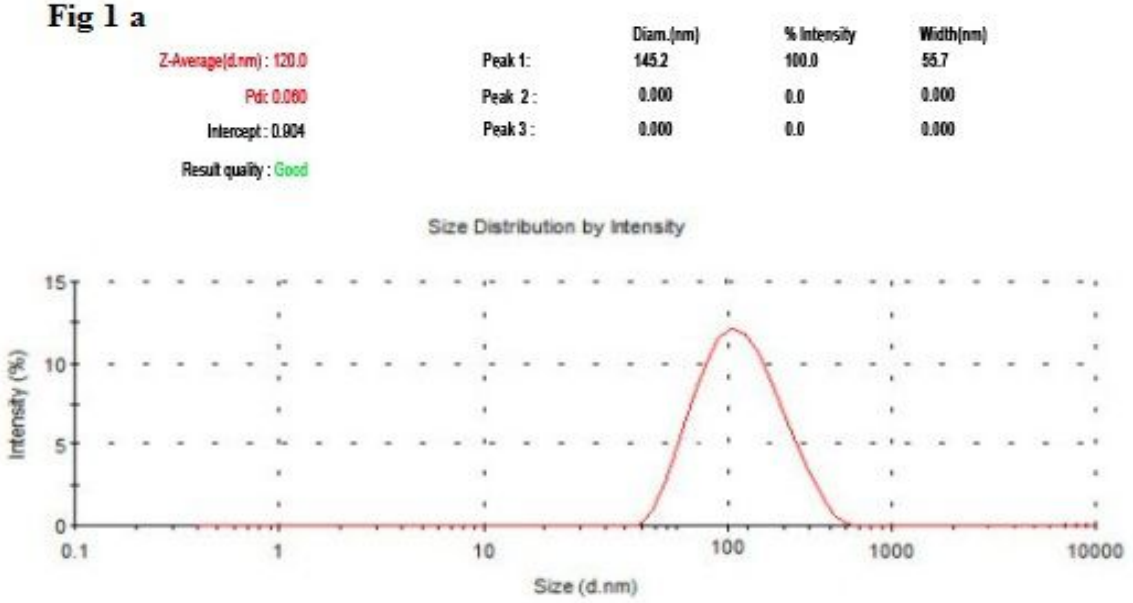

Fig 1 b

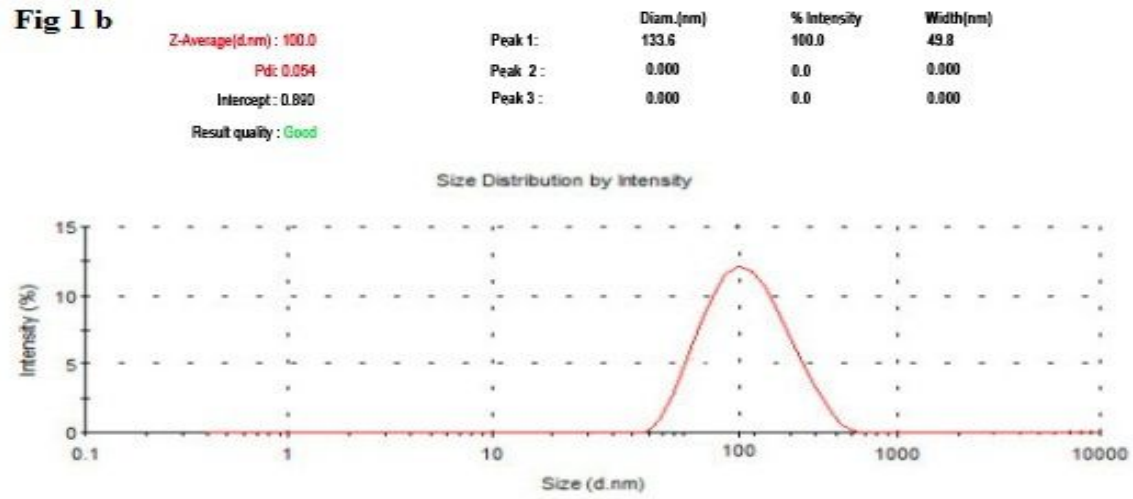

Open Access Journal
International Journal of Medical Research and Pharmaceutical Sciences
Volume 3 (Issue 6) : June 2016 ISSN: 2394-9414
DOI: 10.5281/zenodo.55493 Impact Factor- 3.109

Fig 2

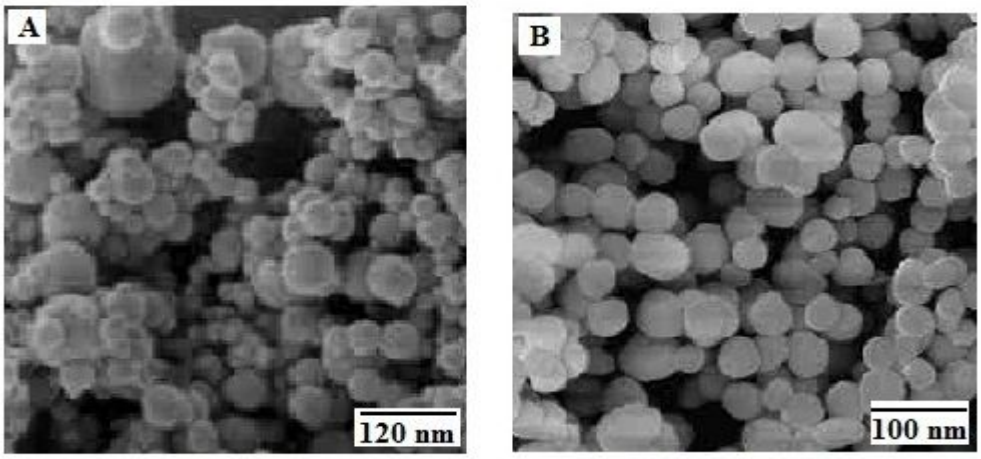

UA - PLGA NPs Caf - PLGA NPs

Fig 3 a

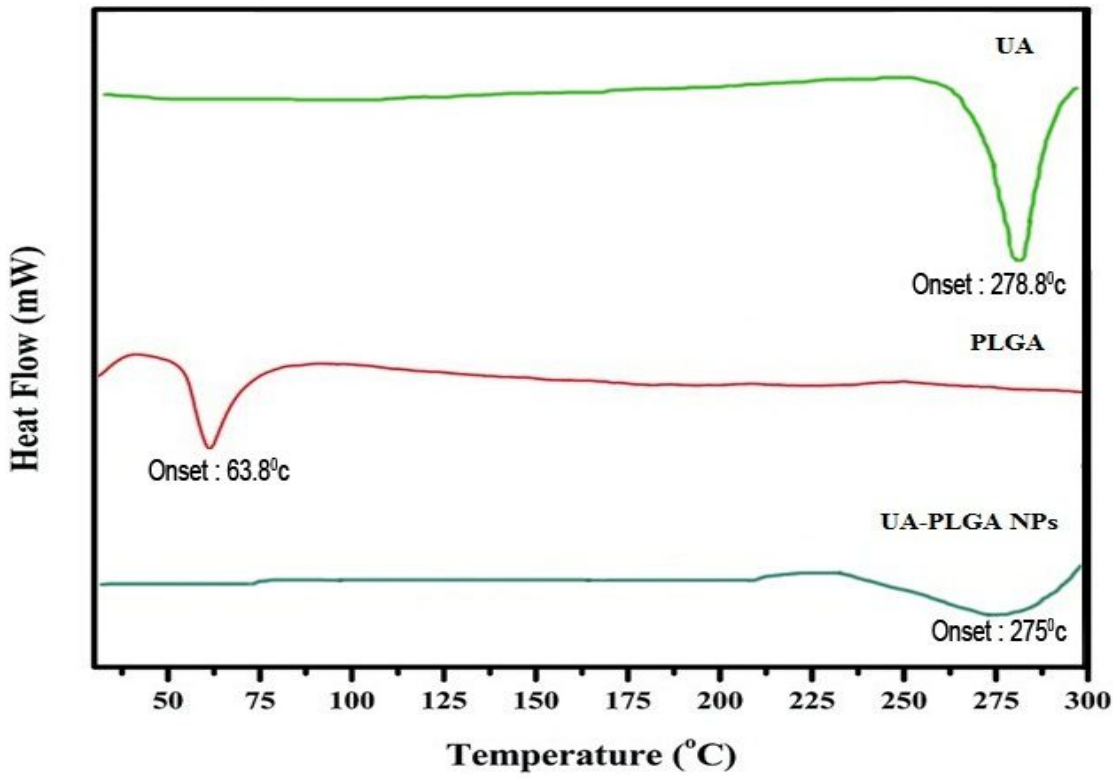

Open Access Journal
International Journal of Medical Research and Pharmaceutical Sciences
Volume 3 (Issue 6) : June 2016 ISSN: 2394-9414
DOI: 10.5281/zenodo.55493 Impact Factor- 3.109

Fig 3 b

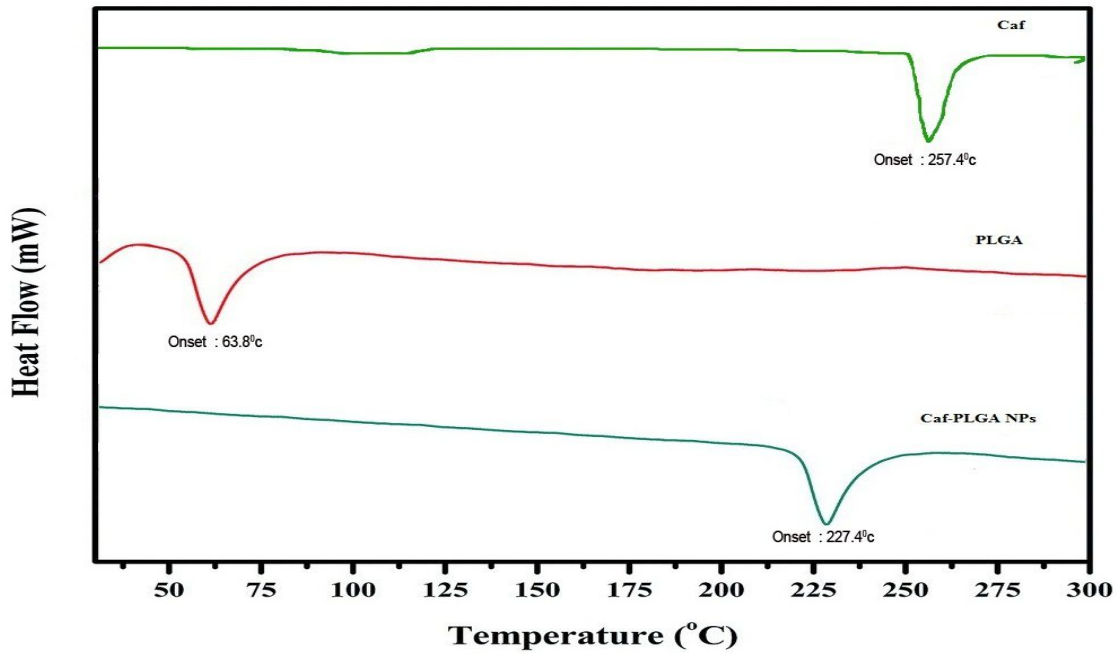

Fig 4

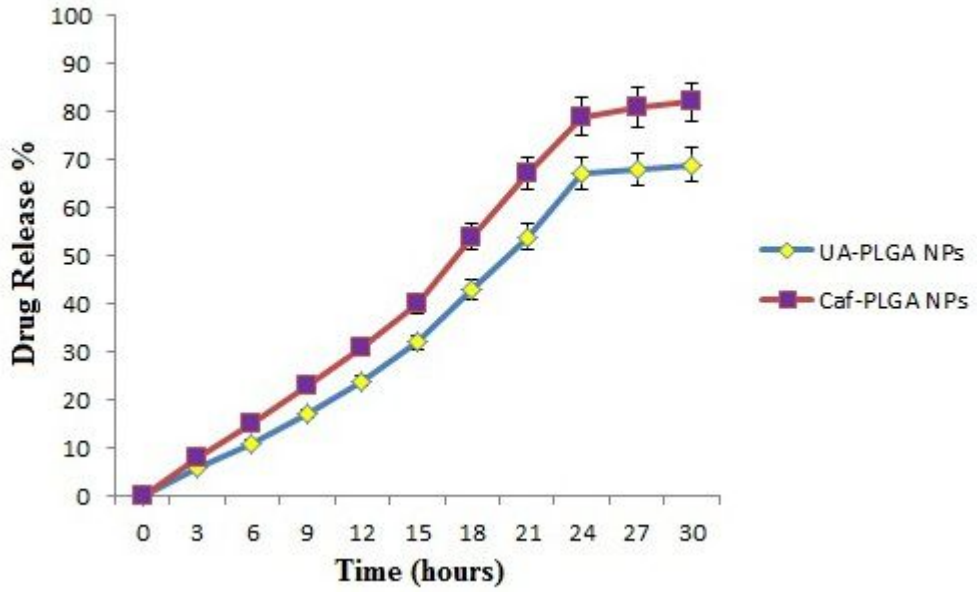

Open Access Journal
International Journal of Medical Research and Pharmaceutical Sciences
Volume 3 (Issue 6) : June 2016 ISSN: 2394-9414
DOI: 10.5281/zenodo.55493 Impact Factor- 3.109

Fig 5

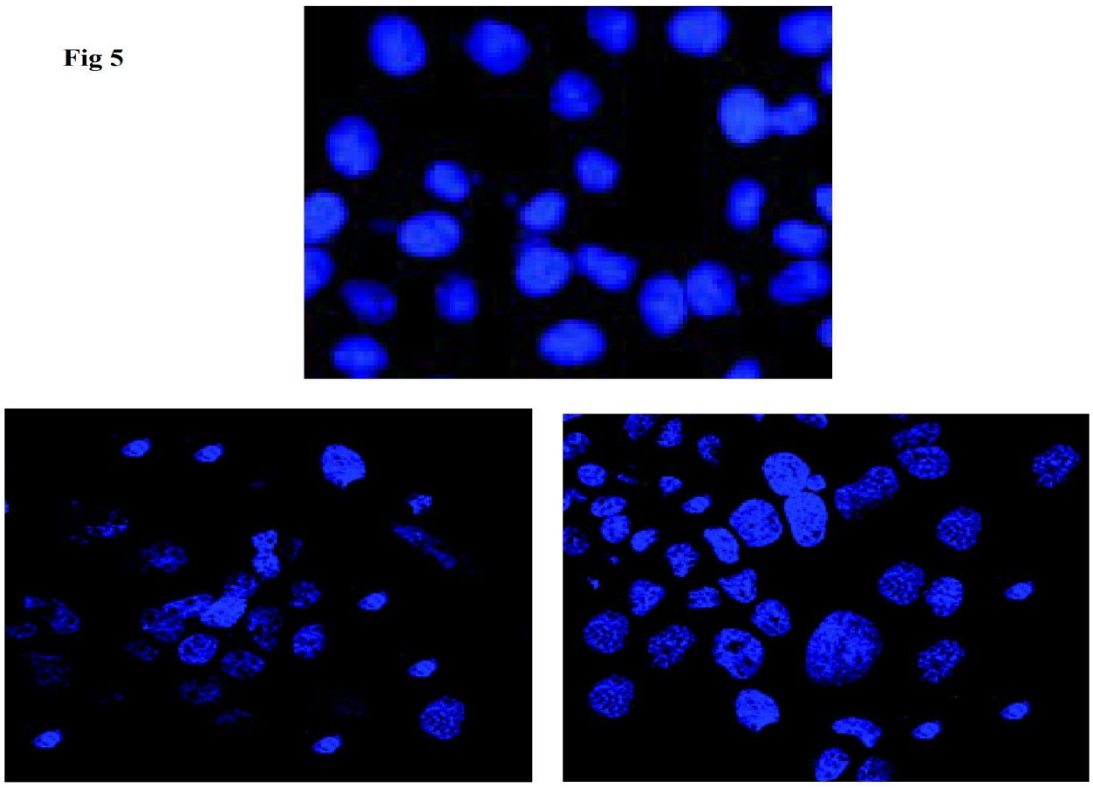

Fig 6

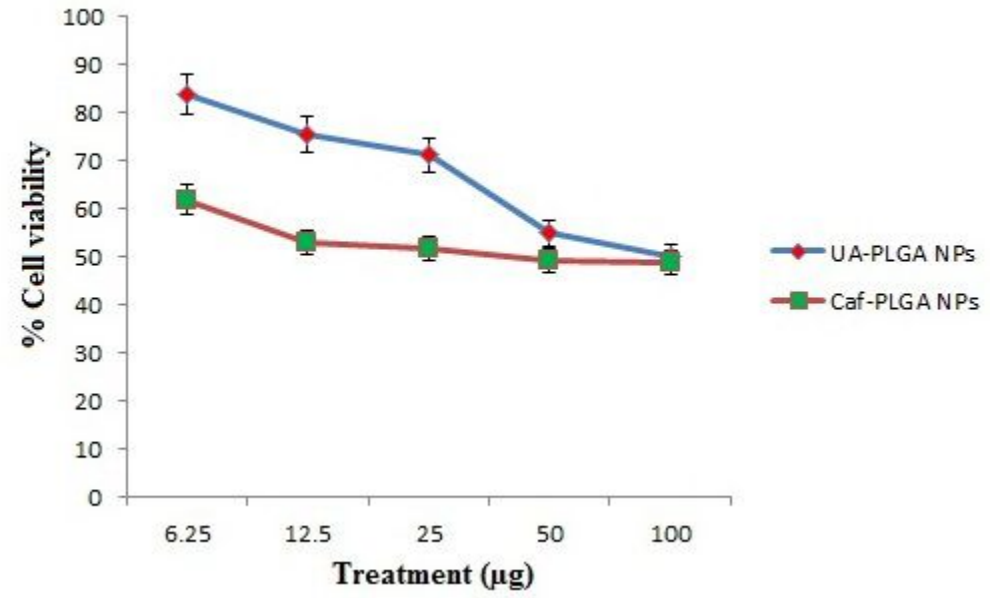

Open Access Journal
International Journal of Medical Research and Pharmaceutical Sciences
Volume 3 (Issue 6) : June 2016 ISSN: 2394-9414
DOI: 10.5281/zenodo.55493 Impact Factor- 3.109

Fig 7 a

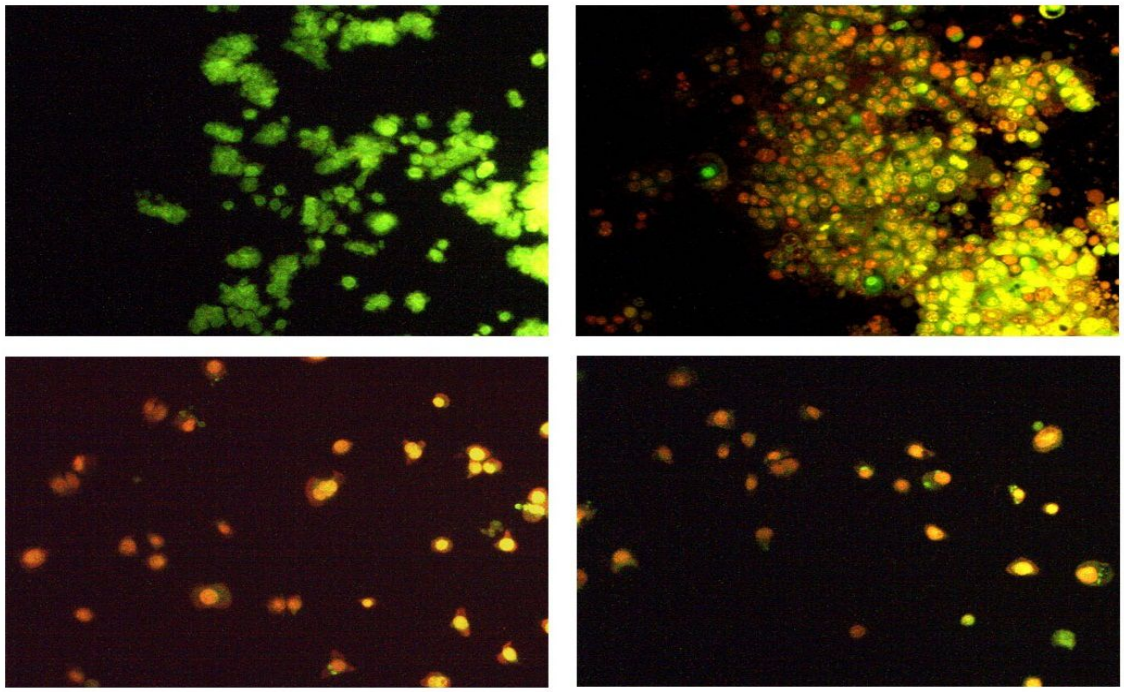

Fig 7 b

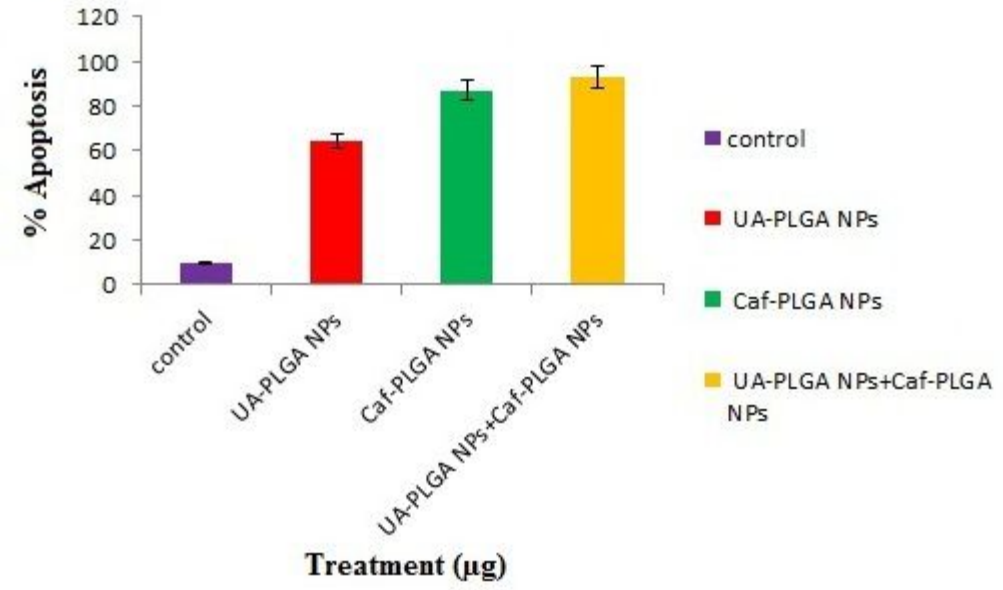

Open Access Journal
International Journal of Medical Research and Pharmaceutical Sciences
Volume 3 (Issue 6) : June 2016 ISSN: 2394-9414
DOI: 10.5281/zenodo.55493 Impact Factor- 3.109

Fig 8